

Membrane scaling and prevention techniques during seawater desalination by air gap membrane distillation

Revised Manuscript Submitted to

Desalination

Hung C. Duong^a, Mikel Duke^b, Stephen Gray^b, Paul Cooper^c, Long D. Nghiem^{a,*}

^a Strategic Water Infrastructure Laboratory, School of Civil Mining and Environmental Engineering, University of Wollongong, Wollongong, NSW 2522, Australia

^b Institute for Sustainability and Innovation, College of Engineering and Science, Victoria University, P.O. Box 14428, Melbourne, Victoria, 8001, Australia

^c Sustainable Buildings Research Centre, University of Wollongong, Fairy Meadow, NSW 2519, Australia

* Corresponding author: Long Duc Nghiem, Email longn@uow.edu.au; Tel: +61 2 4221 4590

Abstract: Membrane scaling and mitigation techniques during air gap membrane distillation (AGMD) of seawater were investigated. The results showed a strong influence of AGMD operating temperature on **not only the process water flux but also membrane scaling and subsequent cleaning efficiency**. Elevating feed/coolant temperature from 35/25 to 60/50 °C **increased** water flux, but also escalated membrane scaling of the AGMD process. Membrane scaling was more severe, and occurred at a lower water recovery (68%) when operating at 60/50 °C compared to 35/25 °C (78%) due to increased concentration polarisation effect. Operating temperature also affected the efficiency of the subsequent membrane cleaning. Membrane scaling that occurred at low temperature (i.e. 35/25 °C) was more efficiently cleaned than at high temperature (i.e. 60/50 °C). In addition, membrane cleaning using vinegar was much more efficient than fresh water. Nevertheless, vinegar cleaning could not completely restore the membrane surface to the original condition. Scaling material remaining on the membrane surface facilitated scaling in the next operation cycle. On the other hand, anti-scalant addition could effectively control scaling. Membrane scaling during AGMD of seawater at 70% water recovery and 60/50 °C was effectively controlled by anti-scalant addition.

Keywords: air gap membrane distillation (AGMD); membrane scaling; membrane cleaning; anti-scalants; polarisation effects; small scale seawater desalination.

1. Introduction

Seawater desalination is a practical approach to secure drinking water supply for coastal communities around the world [1]. Traditional technologies including reverse osmosis (RO) and thermal distillation (e.g. multi-stage flash and multi-effect distillation) are cost-effective for large-scale seawater desalination. However, they are not suitable for small scale applications, particularly where a reliable power supply and technical support are not readily available. RO requires extensive pre-treatment, high-pressure pumps with high and reliable electricity input, and expensive stainless steel components. Conventional thermal distillation technologies are less energy efficient compared to RO. Their physical and energy footprints render them unsuitable for small-scale operations. Given the strategic need for water surety for small coastal communities, several alternative seawater desalination technologies have been explored in recent years. Amongst them, membrane distillation (MD) has emerged as a potential technology platform for small-scale, stand-alone, and off-grid seawater desalination [2-6].

MD is a thermally driven membrane separation process. Unlike RO, MD does not rely on a high hydraulic pressure for mass transfer. [As a result, MD systems can be constructed from inexpensive plastic materials, resulting in considerable cost savings compared to RO that requires stainless steel materials.](#) In addition, the water flux in MD is governed by the water vapour pressure difference between the feed and coolant stream, and is not subjected to osmosis [7, 8]. Thus, seawater desalination using MD can be operated at a higher [feed salinity or process water recovery \(i.e. the volume ratio of total fresh water produced to initial feed water\)](#) compared to RO [9, 10]. Moreover, MD does not require intensive pre-treatment and is less susceptible to organic and colloidal fouling in comparison to RO [11, 12]. Last but not least, given its operating temperature in the range from 40 to 80 °C, MD can directly use waste heat and solar thermal as its main source of energy [13-15]. Given these attributes, MD can be a promising candidate for small-scale and off-grid seawater desalination application in remote coastal areas.

MD can be operated in four basic configurations, including direct contact membrane distillation (DCMD), sweeping gas membrane distillation (SGMD), vacuum membrane distillation (VMD), and air gap membrane distillation (AGMD) [11]. Amongst these configurations, AGMD is arguably the most suitable for a small-scale, energy-efficient seawater desalination process [16-19]. In AGMD, a condenser is inserted between the feed and coolant stream to form an air gap on

the permeate side of the membrane. The inserted condenser allows for the separation between the coolant and distillate stream, hence facilitating the internal recovery of the latent heat of vapour condensation [without the need for an external heat exchanger](#). [By contrast, heat recovery may be possible with other MD configurations \(e.g. DCMD\) but only with an external heat exchanger \[20\]](#). The air gap also functions as an isolation layer to reduce the heat conduction through the membrane from the feed [21]. As a result, AGMD exhibits higher thermal efficiency compared to the other configurations, particularly DCMD. The internal condenser also facilitates water vapour condensation inside the membrane module. Thus, AGMD is less complex than SGMD and VMD, both of which require an external condenser. [It is noteworthy that a variation of AGMD which is often called permeate gap membrane distillation can also be particularly useful for small-scale seawater desalination application in remote areas \[22, 23\]](#).

A key technical challenge to realising MD for small-scale seawater desalination is membrane scaling, which can occur at high water recovery rates. Operating MD at a high water recovery minimises energy loss through the sensible heat of the brine [24]. However, high water recovery operation also increases the risk of membrane scaling caused by the precipitation of sparingly soluble salts in seawater. [Scale layers formed on the membrane can alter the hydrophobicity of the membrane surface, leading to the intrusion of seawater into membrane pores and, thus, deteriorated distillate quality](#). The scale layers also aggravate temperature and polarisation effects and reduce the active membrane surface for water evaporation, hence significantly reducing water flux [25-28].

Several studies have focused on membrane scaling and mitigation techniques during DCMD processes [25, 29-31]. Hickenbottom and Cath [29] demonstrated that intermittently reversing the flow direction of water vapour during DCMD of seawater could effectively sustain water flux even above 75% water recovery. Nghiem and Cath [25] revealed that membrane scaling caused by CaSO_4 during DCMD could be avoided by regularly flushing the membrane with Milli-Q water to reset the induction period. Gryta [30] examined membrane cleaning using a 2–5 wt.% HCl solution for CaCO_3 scaling during a long-term DCMD process of surface water. Membrane cleaning using HCl could fully restore the initial water flux [30]. Recently, anti-scalant addition has proved to be potent in prolonging a DCMD process of seawater RO brine at supersaturation over an extended period of operation [31]. The anti-scalant added to the feed helped delay the precipitation of CaCO_3

and CaSO_4 when they were over-saturated, thus maintaining stability of the water flux and distillate quality of the DCMD process [31].

Membrane scaling and mitigation techniques during AGMD of seawater remain a major research gap. Given a lower operating water flux than DCMD, the scaling behaviour of AGMD can differ from that of DCMD [21, 32]. In addition, most of the aforementioned scaling mitigation techniques are innovative and effective for DCMD, but might not be usable or feasible for a small-scale seawater AGMD process in remote areas. Flow reversal [29] is not compatible to AGMD operation. Similarly, resetting the induction period by regular membrane flushing [25] involves frequent process disruption, which is less preferable for continuously operating desalination systems. Effective membrane cleaning using mineral acids such as HCl and H_2SO_4 has been demonstrated [30, 33]. However, given their corrosive nature, mineral acids cannot be safely stored and used at household level, which is the key target of small-scale seawater AGMD systems. For small-scale seawater AGMD operation in remote areas, non-hazardous and domestically available cleaning agents such as vinegar, which mainly consists of acetic acid (i.e. 5-8 vol.%) and water, are more preferable. To date, no previous study has examined the efficacy of scaling removal during MD operation for seawater desalination by vinegar (i.e. acetic acid).

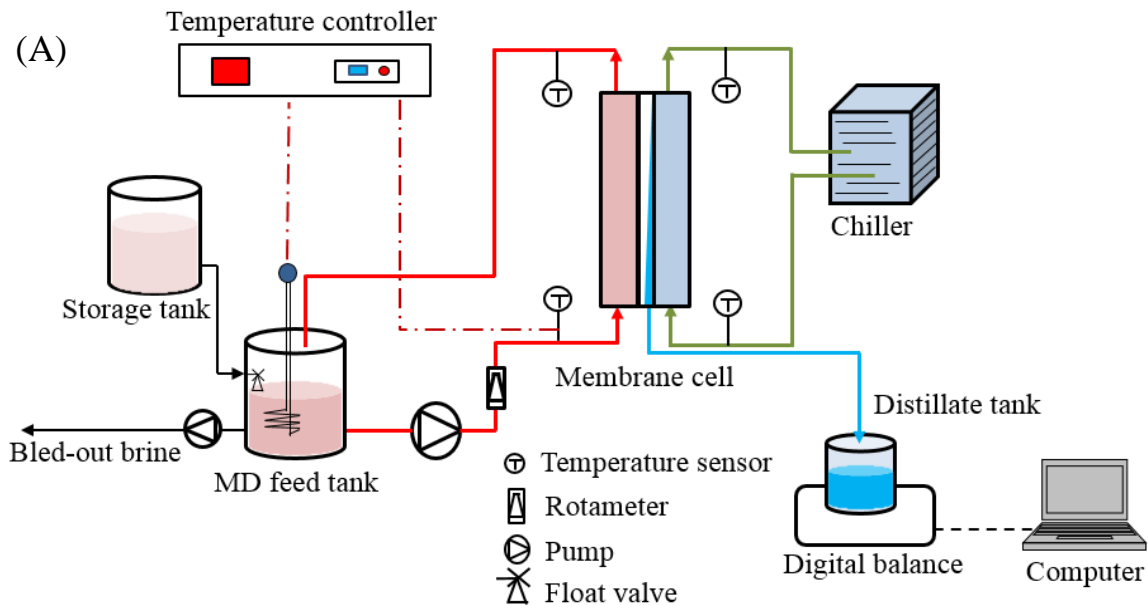
This study aims to elucidate membrane scaling and mitigation techniques during a lab-scale seawater AGMD process operated under conditions practised for small-scale operation. The mass transfer coefficients of the lab-scale AGMD system at different operating temperatures were first experimentally determined. Given the mass transfer coefficients, the influence of feed salinity and particularly membrane scaling on water flux at low and high operating temperature was simulated and then validated by experimental results. In addition, scaling mitigation techniques using a commercially available anti-scalant and vinegar (which is readily available at all households) were also investigated. This study provides important insights for a future pilot study to evaluate AGMD applications for small-scale seawater desalination.

2. Materials and methods

2.1. Materials

2.1.1. AGMD test unit

A lab-scale AGMD system (Fig. 1A) with a plate-and-frame membrane module was used (Fig. 1B). The membrane module consisted of two acrylic semi-cells, an aluminium mesh and an aluminium condenser (0.5 mm thick), rubber gaskets, and spacers. Each semi-cell was engraved to create a flow channel with depth, width, and length of 0.3, 9.5, and 35.0 cm, respectively (Fig. 1B). **Hydrophobic** flat-sheet low-density polyethylene (LDPE) membrane (Aquastill, Sittard, The Netherlands) with nominal pore size, thickness, and porosity of 0.3 μm , 76 μm , and 85%, respectively, was used in all experiments. The aluminium mesh provided support to the membrane and facilitated water vapour condensation on the permeate side, thus increasing water flux of the AGMD system [34]. Rubber gaskets were used to seal the flow channels and to form a 3 mm-thick air gap between the membrane and the condenser. **Polypropylene** spacers (*i.e. with thickness, mesh size, voidage, and hydrodynamic angle of 2.0 mm, 4.0 mm, 0.78, and 60°, respectively*) were used in the feed and coolant channel to increase flow turbulence.



A commercial anti-scalant, Osmotreat OSM35 (Osmoflo Pty Ltd, Adelaide, Australia), was used in the AGMD experiments with seawater at high water recoveries. According to the manufacture, Osmotreat OSM35 contains sodium salt of nitrilotri (methylene) phosphonic acid at 30 – 60 wt.% concentration. This is a widely used anti-scalant ingredient that can inhibit a broad spectrum of scalants, including the sparingly soluble salts of calcium and magnesium.

Fresh water (i.e. TDS = 65 ± 5 mg/L) and a vinegar (from a supermarket) solution with pH of 2.5 ± 0.1 were used to clean the scaled membranes after the AGMD experiments with seawater without anti-scalant addition. Vinegar was chosen as a ‘domestic chemical’ because it is readily available at all households.

2.2. Analytical methods

The contact angle of the membrane surface was measured using a Rame-Hart Goniometer (Model 250, Rame-Hart, Netcong, New Jersey, USA) following the standard sessile drop method (i.e. with the droplet volume of 12 μ L). Milli-Q water was used as the reference liquid. At least 5 droplets were tested for each membrane sample.

The morphology and composition of membrane surface were examined using a low vacuum scanning electron microscope (SEM) coupled with an energy dispersive spectrometer (EDS) (JOEL JSM-6490LV, Japan). Membrane samples were air-dried and subsequently sputtered with a thin layer of gold prior to SEM-EDS analysis.

The electrical conductivity (EC) of the feed and distillate was measured using Orion 4-Star Plus meters (Thermo Scientific, Waltham, Massachusetts, USA).

2.3. Experimental protocols

2.3.1. AGMD with Milli-Q water and seawater

AGMD of Milli-Q water was conducted to determine the baseline mass transfer coefficient of the system prior to experiments using seawater. The process was operated at a constant water circulation rate of 0.5 L/min (i.e. equivalent to a cross flow velocity of 0.03 m/s given the cross sectional area of the flow channels of 2.8×10^{-4} m²) and temperature difference between the feed and the coolant stream ($\Delta T = 10$ °C), but with various feed/coolant temperature (i.e. 35/25, 40/30,

45/35, 50/40, 55/45, and 60/50 °C). Water flux was measured at each pair of feed/coolant temperatures following the attainment of stable operation for 1 hour. The operating conditions were chosen to simulate a small-scale AGMD process [16, 21, 32], in which feed and coolant temperatures vary while ΔT and water circulation rates are almost constant along membrane channels.

AGMD of seawater was operated at two pairs of temperature conditions (e.g. 35/25 and 60/50 °C), with water circulation rates of 0.5 L/min. Milli-Q water (1 L) was initially added to the distillate tank to allow the immediate measurement of the distillate conductivity after starting the AGMD process. The seawater feed (4 L) was continuously concentrated until the process reached a water recovery of 80% (i.e. concentration factor of 5) or water flux decreased to zero. Water flux was monitored continuously along with the electrical conductivity of the feed and the distillate. At the end of the experiments, the membrane was removed for subsequent surface analyses.

2.3.2. AGMD of seawater with anti-scalant

AGMD process of seawater at a high water recovery was conducted with Osmotreat OSM35 at a dose of 0.5 mg/L to demonstrate the effectiveness of anti-scalant for membrane scaling prevention. The feed solution (4 L) was first concentrated until the process reached 70% water recovery (i.e. the feed solution volume was reduced to 1.2 L), then a continuous operation mode was initiated. The detailed description of the continuous operation mode can be found elsewhere [24].

2.3.3. Membrane cleaning during AGMD of seawater

AGMD of seawater without anti-scalant was first conducted under the same operating conditions as described in the section 2.3.1. At the end of the process, instead of removing the scaled membrane for surface analysis, membrane cleaning using either fresh water or vinegar was initiated. The cleaning solution (2 L) was circulated through the feed channel at 0.5 L/min for one hour at room temperature (25 °C). After membrane cleaning with vinegar, the feed channel was rinsed with 2 L of fresh water for 5 minutes. The efficiency of membrane cleaning was evaluated based on the restorations of initial membrane hydrophobicity and water flux, and the distillate quality of the subsequent AGMD process with seawater using the cleaned membrane. SEM-EDS analysis of membrane surface was also used for the evaluation of cleaning efficiency.

2.4. Mass transfer of water in AGMD

In AGMD, water vapour from the feed is transported through membrane pores and subsequently condenses to distillate on the condenser surface at the other end of the air gap. The water flux of the AGMD system can be expressed as [35-37]:

$$J = K_m \Delta P \quad (1)$$

where J is in L/m².h, K_m is the system mass transfer coefficient (L/m².h.Pa), and ΔP is the water vapour pressure difference between the feed and coolant stream (Pa). The value of K_m depends on system specifications (e.g. the properties of the membrane, the aluminium mesh and condenser, and the air gap thickness) and operating conditions (e.g. feed and coolant temperature and circulation rates, and the pressure of the air gap). Thus, K_m is a system-specific parameter, and it can be determined experimentally. K_m is a useful and convenient coefficient to assess mass transfer [38].

The water vapour pressure difference between the seawater feed and coolant stream can be calculated as [38]:

$$\Delta P = x_{water} \left(1 - 0.5x_{salt} - 10x_{salt}^2 \right) P_{feed}^0 - P_{coolant}^0 \quad (2)$$

where x_{water} and x_{salt} are the molar fraction of water and salt in the feed, P_{feed}^0 and $P_{coolant}^0$ (Pa) are the vapour pressure of pure water in the feed and the coolant stream, respectively. The vapour pressure of pure water can be calculated using the Antoine Equation [39]:

$$P^0 = \exp \left(23.1964 - \frac{3816.44}{T - 46.13} \right) \quad (3)$$

where T is the absolute water temperature (K). The temperatures of the feed and coolant stream were the average values of the temperatures at the inlet and outlet of the feed and the coolant channel, respectively.

3. Results and discussions

3.1. Baseline testing of the AGMD process with Milli-Q water feed

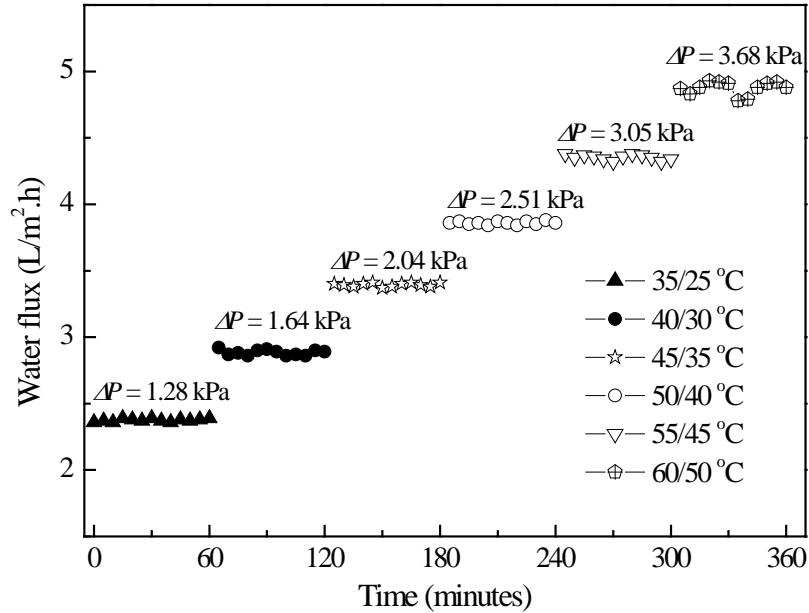


Fig. 2. Experimentally measured water flux during the AGMD process with Milli-Q water feed at various feed/coolant temperature, a constant ΔT of 10 °C, and water circulation rates $F_{feed.in} = F_{coolant.in} = 0.5$ L/min.

Operating the AGMD process at a high feed temperature while maintaining the same temperature difference between the feed and coolant stream (ΔT) resulted in a marked increase in the process water flux (Fig. 2). Given the exponential relationship between water vapour pressure and temperature as expressed in Eq. (3), increasing the feed/coolant temperature from 35/25 to 60/50 °C raised the water vapour pressure difference between the feed and the coolant stream (ΔP) from 1.28 to 3.68 kPa. As a result, water flux almost doubled when the feed/coolant temperature increased from 35/25 to 60/50 °C. Varying feed/coolant temperature also exerted a small but discernible influence on the mass transfer coefficient (K_m) of the AGMD process (Table 1). Increasing both feed and coolant temperatures while other operating parameters remained unchanged resulted in a reduction in K_m . The observed decrease in K_m was attributed to the temperature polarisation effect which was incorporated in the determination of K_m . Operating the

process at increased water flux by elevating feed/coolant temperature escalated temperature polarisation effect as expressed by Eq. (4) [36]:

$$\theta = 1 - \alpha(1 - e^{-\beta J}) \quad (4)$$

where θ is the temperature polarisation coefficient (i.e. approaches to unity for the process without temperature polarisation effect), α and β are constants depending on heat transfer coefficients of the process. Temperature polarisation effect led to a decrease in the actual driving force of the AGMD process, thus reducing the value of K_m obtained.

Table 1. The mass transfer coefficient of the AGMD process with Milli-Q water feed at various feed/coolant temperature.

Feed/coolant temperature (°C)	Mass transfer coefficient, $K_m \times 10^3$ (L/m ² .h.Pa)
35-25	1.84
40-30	1.75
45-35	1.66
50-40	1.54
55-45	1.42
60-50	1.31

The results reported here reveal an uneven distribution of water flux and hence distillate production along the membrane channels of a small-scale AGMD module. For a long membrane channel, a significant drop in feed temperature and an increase at the same magnitude in coolant temperature are expected over the AGMD membrane module [16, 21, 32]. Higher water flux and more distillate can be obtained at the high temperature end compared to the low temperature end of the membrane module. Thus, the high temperature end is more susceptible to membrane scaling, and this uneven distribution should be considered during membrane module design.

3.2. AGMD of seawater

The K_m values reported in Table 1 were valid for the AGMD process with Milli-Q water feed in which concentration polarisation effect was negligible. [These values could be used for a preliminary evaluation of the influence of increased feed salinity on water flux.](#) As the seawater feed was concentrated and the recovery of distillate increased, a linear decrease in AGMD water flux was expected based on mathematical simulation (Fig. 3A). According to Eq. 2, increasing feed salinity leads to a reduction in the water vapour pressure of the feed, and thus a decrease in the

driving force (ΔP) of AGMD. As a result, water flux decreased when seawater was concentrated. It is noteworthy that the impact of feed salinity on water flux in AGMD is much less significant compared to that observed in RO [40]. When the seawater feed was concentrated by 5-fold (i.e. 80% water recovery), the calculated AGMD water flux decreased by 45% and 30% at feed/coolant temperature of 60/50 and 35/25 °C, respectively (Fig. 3A).

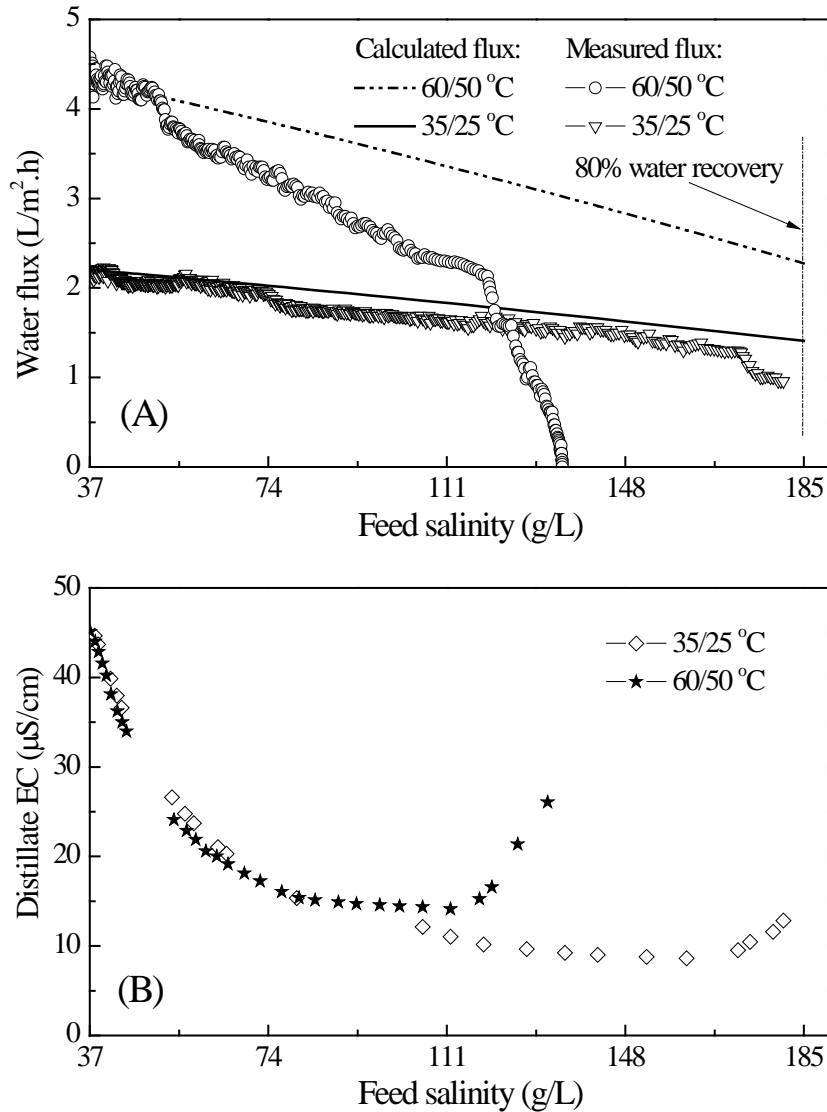


Fig. 3. (A) Calculated and experimentally measured water flux and (B) Distillate electrical conductivity (EC) as functions of feed salinity during the concentrating AGMD process with seawater feed. Water circulation rates $F_{feed.in} = F_{coolant.in} = 0.5$ L/min.

The experimentally measured water flux of the AGMD process with seawater feed also decreased during the concentration of the feed as observed with the calculated flux. However, the measured flux deviated from the calculated values, especially at high feed salinity (Fig. 3A). This deviation can be attributed to concentration polarisation effect and membrane scaling caused by sparingly soluble salts in the seawater feed. The K_m values used for water flux calculation were obtained during the AGMD process with Milli-Q water feed without concentration polarisation effect. For the AGMD process with seawater, concentration polarisation effect can be expressed by Eq. (5) [41]:

$$\frac{C_{m,feed}}{C_{b,feed}} = \exp\left(\frac{J}{k}\right) \quad (5)$$

where $C_{m,feed}$ and $C_{b,feed}$ are the salt concentration at the membrane surface and in the bulk solution in the feed channel, respectively, and k is the mass transfer coefficient of salt. Increase in feed viscosity associated with increased feed salinity [31, 42] during the concentration of the seawater feed reduced k , thus exacerbating concentration polarisation effect. Increased water flux also exacerbated concentration polarisation effect. As a result, the experimentally measured water flux deviated more from the calculated values at higher feed salinity and feed temperature (Fig. 3A).

The precipitation of sparingly soluble salts on the membrane surface when their concentrations exceeded saturation limits further reduced the measured water flux. The deposited salts on the membrane promoted temperature and concentration polarisation [26], and reduced partial water vapour pressure on the membrane surface [43, 44] and the membrane active surface for water evaporation [7, 25], thus decreasing water flux. Indeed, the measured water flux rapidly decreased from 2.5 L/m².h to almost zero and from 1.5 to 0.9 L/m².h as the feed salinity exceeded 115 and 170 g/L (i.e. water recovery of 68% and 78%) at feed/coolant temperature of 60/50 and 35/25 °C, respectively (Fig. 3A).

The scale layers formed on the membrane surface also deteriorated the distillate purity. Prior to the onset of membrane scaling, the distillate conductivity gradually decreased owing to the dilution of the initially added Milli-Q water by the distillate permeating from the feed (Fig. 3B). The observed decline in the distillate conductivity revealed that the AGMD process could produce ultrapure distillate (i.e. with electrical conductivity significantly lower than that of Milli-Q water)

directly from seawater. Scales deposited on the membrane surface led to a rapid decline in the pure distillate flux, whereas salt leakage through the membrane defects was unchanged. In addition, the scaling layer could alter the membrane surface hydrophobicity [28, 30, 45], resulting in some salt leakage and thus increasing the distillate conductivity. As a result, the reversal of the distillate conductivity coincided with the significant decline in the water flux (Fig. 3).

Membrane surface analyses confirmed the occurrence of membrane scaling during the concentrating AGMD process with seawater (Fig. 4). SEM images showed thick layers of well-shaped salt crystals formed on the membrane surface. The EDS elemental analyses revealed that the scale layers were composed of mostly CaSO_4 and MgSO_4 . These results are consistent with previous studies by Duong et al. [24] and Zhang et al. [31]. Moreover, the scale layers rendered the membrane surface so hydrophilic that its water contact angle could not be determined by the standard sessile drop method.

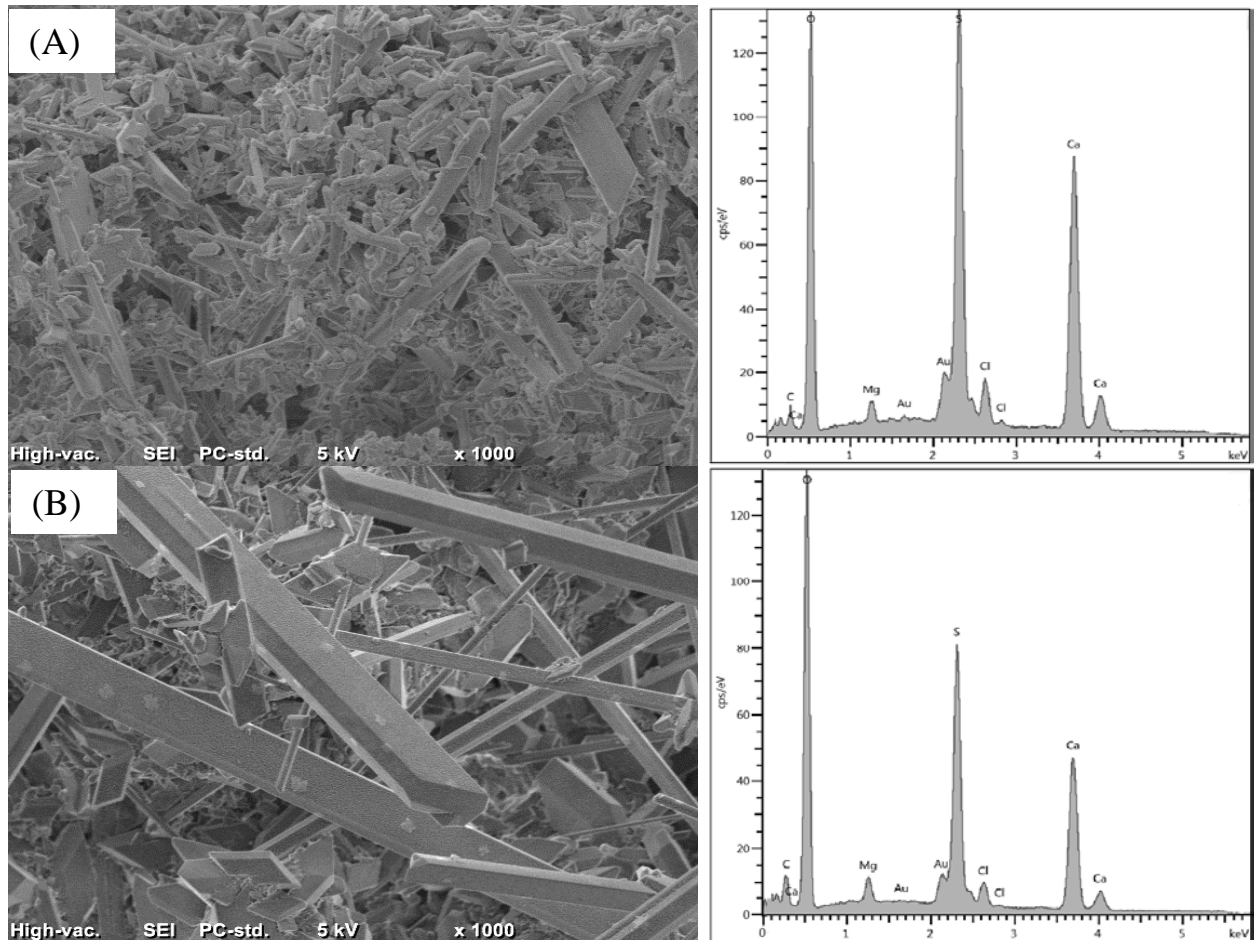


Fig. 4. SEM images and EDS spectra of the scaled membranes after the concentrating AGMD operations with seawater feed at feed/coolant temperature of: (A) 35/25 °C and (B) 60/50 °C.

Operating temperature exerted a strong influence on membrane scaling of AGMD with the seawater feed. Elevating feed/coolant temperature exacerbated concentration polarisation effect and depressed the solubility of CaSO₄, thus aggravating membrane scaling. As a result, membrane scaling occurred at a lower feed salinity (i.e. lower water recovery) for feed/coolant temperature of 60/50 °C compared to 35/25 °C (Fig. 3A&B). Operating temperature also affected the morphologies of the scale layers; larger and more needle-shaped crystals were formed on the membrane surface during the AGMD experiment at 60/50 °C compared to 35/25 °C (Fig. 4). These results are consistent with the scaling study by Nghiem et al. [25] in which increasing feed temperature also favoured the formation of large CaSO₄ crystals during DCMD. The cause and effect relationships between elevating feed/coolant temperature and aggravated membrane scaling of the AGMD process are summarised in Table 2.

Table 2. The cause and effect relationships between elevating temperature and aggravated membrane scaling during AGMD with seawater.

Cause	Effect
Increasing feed/coolant temperature	Increased water flux
Increased water flux	Exacerbated polarisation effects
Exacerbated concentration polarisation	Increased CaSO ₄ concentrations at the membrane surface
Exacerbated temperature polarisation	Decreased solubility of CaSO ₄
Exacerbated polarisation effects	Aggravated membrane scaling
Aggravated membrane scaling	Scaling occurred at lower water recovery
Aggravated membrane scaling	Larger and more needle-shaped scales

3.3. AGMD of seawater with anti-scalant addition at a high water recovery

Anti-scalant addition proved to be an effective method to prevent membrane scaling during AGMD of seawater. A stable AGMD process (i.e. with respect to water flux and distillate conductivity) with seawater feed dosed with 0.5 mg/L Osmotreat OSM35 at the water recovery of 70% and feed/coolant temperature of 60/50 °C was achieved for 24 hours without any observable membrane scaling. Water flux was stable at 2.5 L/m².h following an initial gradual decrease because of increased feed salinity during the concentrating operation (Fig. 5). Distillate

conductivity exhibited a similar trend to water flux. SEM analysis (Fig. 6) also revealed no indications of membrane scaling—the SEM surface image of the membrane at the end of the continuous operation was identical to that of a virgin membrane. Anti-scalants have been investigated for membrane scaling prevention in DCMD processes [31, 46-48]. Zhang et al. [31] reported that an anti-scalant dose of 5.0 mg/L effectively prevented scale formation during a DCMD process of a seawater RO brine with electrical conductivity of 120 mS/cm (i.e. corresponding to a water recovery of 65% relative to the seawater in this study). It is noteworthy that the lower water flux and hence lower polarisation effects of the AGMD process compared to the DCMD process previously investigated by Zhang et al. [31] could also help alleviate membrane scaling at 70% water recovery obtained in this study.

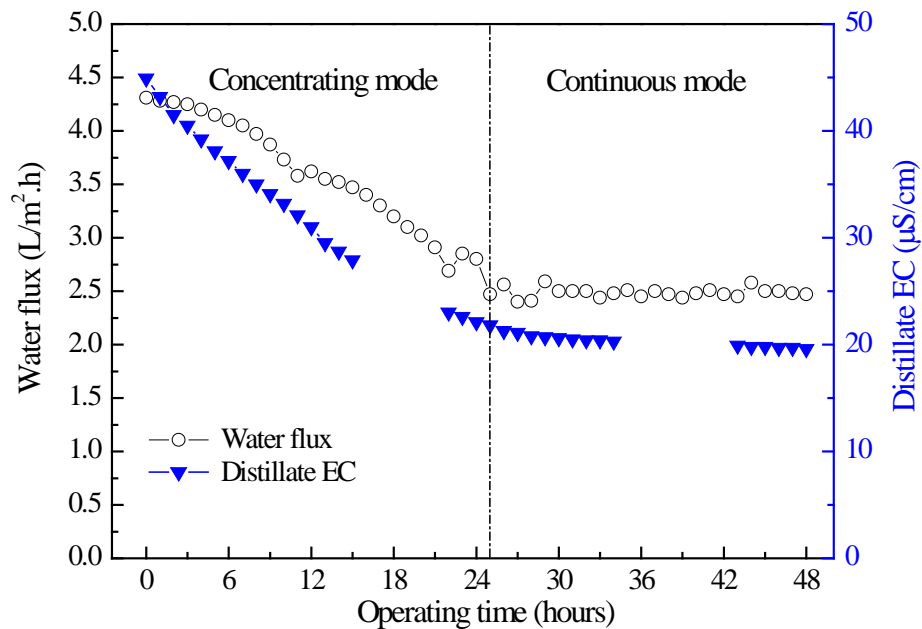


Fig. 5. Water flux and distillate EC as functions of operating time during the AGMD process of seawater dosed with 0.5 mg/L Osmotreat OSM35.

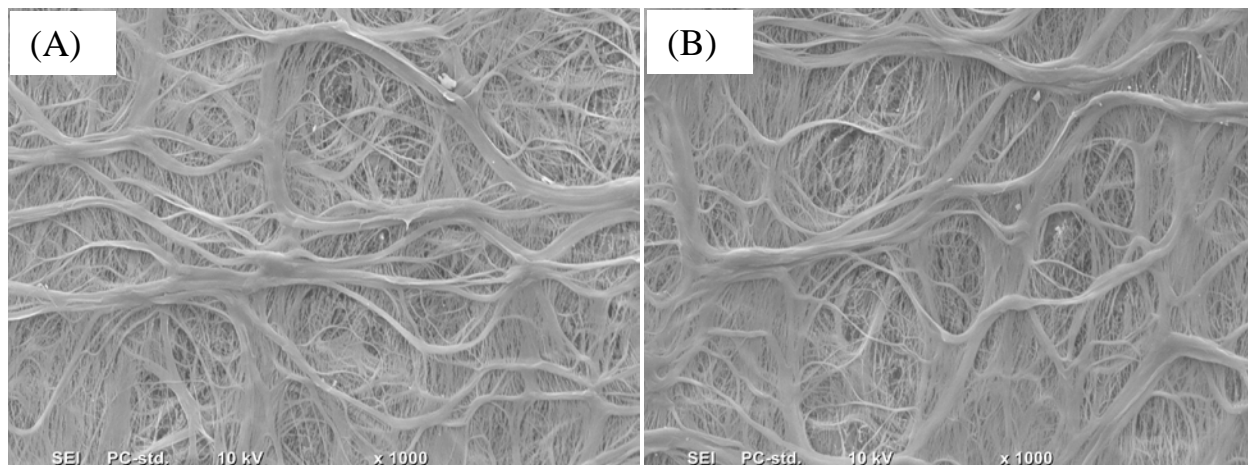


Fig. 6. SEM images of (A) a virgin membrane and (B) the membrane after the AGMD process of seawater dosed with 0.5 g/L Osmotreat OSM35 at 60/50 °C.

The results reported here demonstrate the potential of seawater AGMD desalination for fresh water provision in small and remote areas. Given water flux of 2.5 L/m².h even at process water recovery of 70%, a pilot-scale AGMD system with membrane surface area of 7.2 m² [19, 21] can provide 144 L of distillate for eight hours during daytime. The heating requirement of the system can be sourced from solar thermal energy while cooling can be achieved using seawater as a heat sink [21]. Compared to thermal energy requirement, the electrical energy consumption of the AGMD system is negligible. A comprehensive techno-economic analysis is required to determine the cost and energy consumption of seawater desalination by AGMD. However, such analysis is beyond the scope of this current work.

3.4. Efficiency of membrane cleaning during AGMD of seawater

Vinegar demonstrated higher cleaning efficiency compared to fresh water under the same AGMD operating and cleaning conditions. Fresh water cleaning was not able to restore membrane surfaces to their original conditions. SEM analyses revealed many tiny, dispersed particles remaining on the membrane surface after fresh water cleaning (Fig. 7). The remaining particles altered the hydrophobicity of the membrane surface, thus rendering the membrane surface slightly hydrophilic (i.e. contact angles below 80°) (Fig. 8). In contrast, vinegar cleaning returned the membrane surface to an almost virgin condition as had been demonstrated for mineral acidic cleaning agents [30]. The SEM image of the vinegar cleaned membrane after AGMD of seawater at 35/25 °C was similar to that of the virgin membrane, and only traces of salts remained on the

membrane surface following vinegar cleaning of the membrane scaled at 60/50 °C (Fig. 7). In a good agreement with SEM analyses, the surface of the scaled membranes after vinegar cleaning was still hydrophobic (i.e. contact angles above 90°) (Fig. 8). It is noteworthy that the differences in contact angles of the virgin and vinegar cleaned membranes (Fig. 8) may not be solely attributed to membrane scaling. Decline in membrane contact angle has been reported for an MD process of fresh water without any membrane scaling [49].

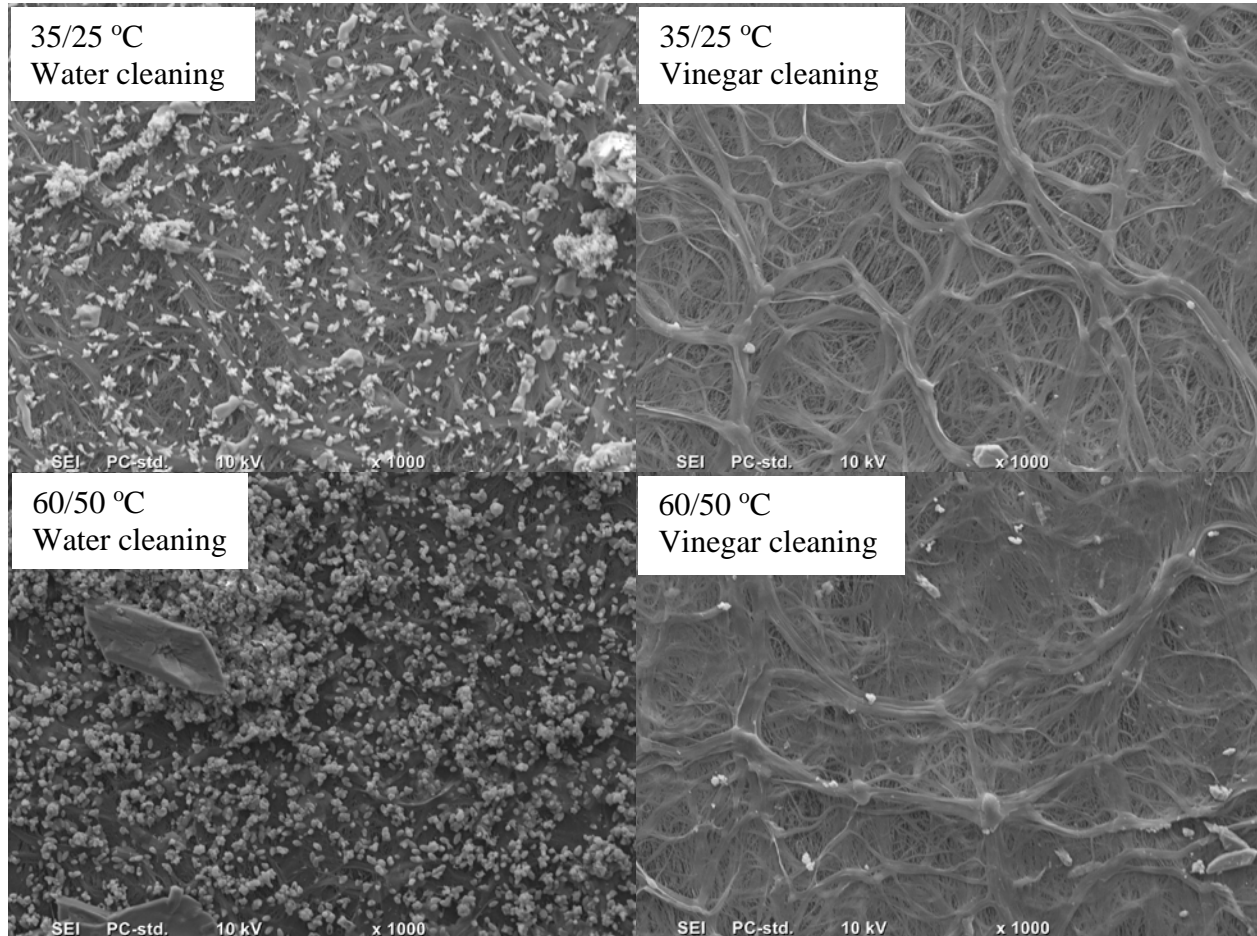


Fig. 7. SEM images of the scaled membranes at 35/25 and 60/50 °C after cleaning with fresh water and vinegar.

AGMD operating temperature affected not only membrane scaling (section 3.2), but also the efficiency of subsequent membrane cleaning. SEM images (Fig. 7) and contact angle measurements (Fig. 8) revealed that cleaning was less effective for the membrane scaled at 60/50 °C compared to that at 35/25 °C. The variation in cleaning efficiency can be attributed to the difference in the conditions under which membrane scaling occurred. Membrane scaling at 60/50

°C was more severe than that at 35/25 °C due to the increased concentration polarisation effect [9, 29] and saturation index of the scalants, particularly CaSO₄ [50]. The influence of operating conditions on the morphology of scale layers has also been reported by Gryta [51]. Scale layers formed during DCMD with surface water feed were more compact when operating at higher water circulation rate [51].

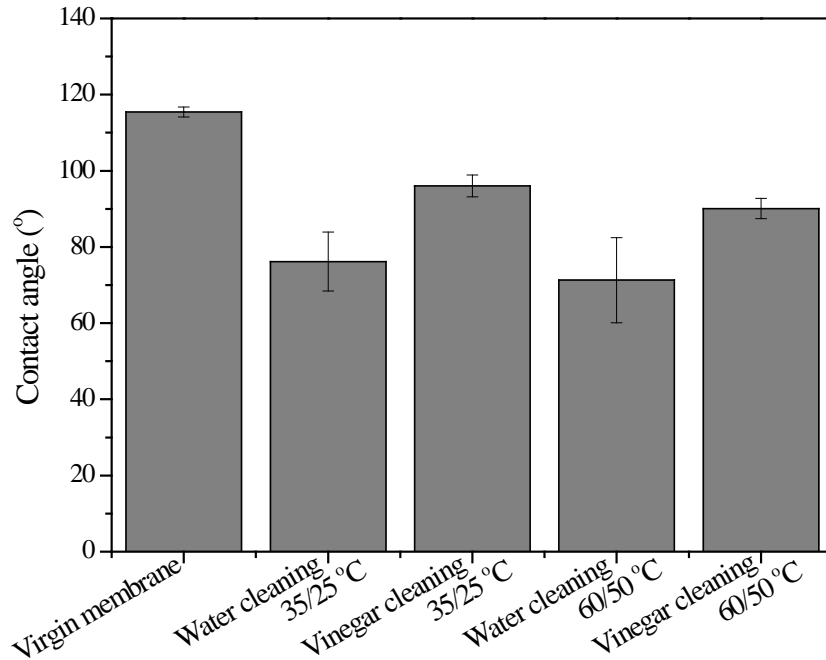


Fig. 8. Contact angles of the virgin membrane and the scaled membranes at 35/25 and 60/50 °C after cleaning with fresh water and vinegar. Error bars represent the standard deviation of 5 repeated measurements.

Despite demonstrating a superior efficiency than fresh water, vinegar cleaning could not fully restore the performance of the AGMD process, particularly at high operating temperature. Fig. 9 shows water flux and distillate conductivity during the AGMD operation with seawater feed at 60/50 °C before and after one vinegar cleaning cycle. The initial water flux of the AGMD process (i.e. with fresh seawater feed) was almost fully recovered after membrane cleaning with vinegar. However, membrane scaling occurred at a lower water recovery in the AGMD process following vinegar cleaning. The remnants of scale on the membrane surface (Fig. 7) acted as nuclei for scale decomposition [9, 31], and promoted the concentration and temperature polarisation effects [26], thus aggravating membrane scaling in the subsequent AGMD process. The results reported here

indicate that repeated membrane scaling and cleaning during AGMD of seawater inevitably result in decrease in process performance. Thus, anti-scalant addition is preferable to membrane cleaning, and membrane cleaning should only be used as the last resort for scaling mitigation in AGMD of seawater.

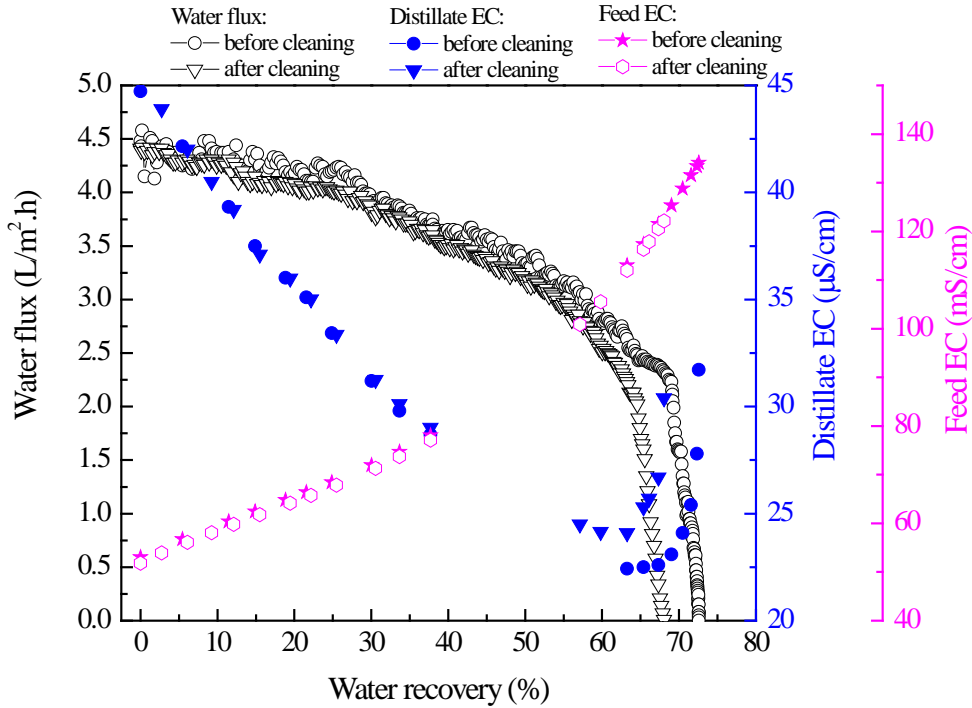


Fig. 9. Water flux, distillate EC, and feed EC as functions of water recovery during AGMD with seawater feed before and after one membrane cleaning cycle with vinegar. Operating parameters: feed/coolant temperature of 60/50 °C, water circulation rates $F_{feed.in} = F_{coolant.in} = 0.5$ L/min.

4. Conclusions

Membrane scaling and mitigation techniques during AGMD of seawater were investigated. The results demonstrated a clear impact of feed/coolant temperature on both water flux and scaling behaviours of the AGMD process with seawater. At feed/coolant temperature of 60/50 °C, the water flux was double compared to that at feed/coolant temperature of 35/25 °C. Membrane scaling occurred at a lower water recovery and resulted in needle-shaped and larger crystals at 60/50 °C compared to 35/25 °C. Operating temperature also affected the effectiveness of the subsequent scaled membrane cleaning. Membrane cleaning was less effective for the membrane scaled at

higher feed/coolant temperature. [Vinegar cleaning allowed for complete restoration of the initial water flux](#). Nonetheless, vinegar cleaning could not completely remove all scalants from the membrane surface. Anti-scalant addition was an effective scaling mitigation technique for seawater AGMD. Stable AGMD operation was achieved over 24 hours without any sights of membrane scaling when seawater was dosed with 0.5 g/L anti-scalant, the water recovery was constant at 70%, and the feed/coolant temperature was 60/50 °C.

References

- [1] M. Elimelech and W.A. Phillip, The Future of Seawater Desalination: Energy, Technology, and the Environment, *Science* 333 (2011) 712-717.
- [2] G. Zaragoza, A. Ruiz-Aguirre, and E. Guillén-Burrieza, Efficiency in the use of solar thermal energy of small membrane desalination systems for decentralized water production, *Appl. Energy* 130 (2014) 491-499.
- [3] A. Chafidz, S. Al-Zahrani, M.N. Al-Otaibi, C.F. Hoong, T.F. Lai, and M. Prabu, Portable and integrated solar-driven desalination system using membrane distillation for arid remote areas in Saudi Arabia, *Desalination* 345 (2014) 36-49.
- [4] J. Koschikowski, M. Wieghaus, and M. Rommel, Solar thermal-driven desalination plants based on membrane distillation, *Desalination* 156 (2003) 295-304.
- [5] J.-P. Mericq, S. Laborie, and C. Cabassud, Evaluation of systems coupling vacuum membrane distillation and solar energy for seawater desalination, *Chem. Eng. J.* 166 (2011) 596-606.
- [6] B. Bolto, T. Tran, and M. Hoang, Membrane distillation - A low energy desalting technique?, *Water* 34 (2007) 59-62.
- [7] L.D. Nghiem, F. Hildinger, F.I. Hai, and T. Cath, Treatment of saline aqueous solutions using direct contact membrane distillation, *Desalin. Water Treat.* 32 (2011) 234-241.
- [8] S. Adham, A. Hussain, J.M. Matar, R. Does, and A. Janson, Application of membrane distillation for desalting brines from thermal desalination plants, *Desalination* 314 (2013) 101-108.
- [9] H.C. Duong, M. Duke, S. Gray, T.Y. Cath, and L.D. Nghiem, Scaling control during membrane distillation of coal seam gas reverse osmosis brine, *J. Membr. Sci.* 493 (2015) 673-682.
- [10] S. Lin, N.Y. Yip, and M. Elimelech, Direct contact membrane distillation with heat recovery: Thermodynamic insights from module scale modeling, *J. Membr. Sci.* 453 (2014) 498-515.

- [11] E. Drioli, A. Ali, and F. Macedonio, Membrane distillation: Recent developments and perspectives, *Desalination* 356 (2015) 56-84.
- [12] J. Koschikowski, M. Wieghaus, M. Rommel, V.S. Ortin, B.P. Suarez, and J.R. Betancort Rodríguez, Experimental investigations on solar driven stand-alone membrane distillation systems for remote areas, *Desalination* 248 (2009) 125-131.
- [13] N. Dow, S. Gray, J.-d. Li, J. Zhang, E. Ostarcevic, A. Liubinas, P. Atherton, G. Roeszler, A. Gibbs, and M. Duke, Pilot trial of membrane distillation driven by low grade waste heat: Membrane fouling and energy assessment, *Desalination* 391 (2016) 30-42.
- [14] W.G. Shim, K. He, S. Gray, and I.S. Moon, Solar energy assisted direct contact membrane distillation (DCMD) process for seawater desalination, *Sep. Purif. Technol.* 143 (2015) 94-104.
- [15] N. Ghaffour, J. Bundschuh, H. Mahmoudi, and M.F.A. Goosen, Renewable energy-driven desalination technologies: A comprehensive review on challenges and potential applications of integrated systems, *Desalination* 356 (2015) 94-114.
- [16] E. Guillén-Burrieza, G. Zaragoza, S. Miralles-Cuevas, and J. Blanco, Experimental evaluation of two pilot-scale membrane distillation modules used for solar desalination, *J. Membr. Sci.* 409–410 (2012) 264-275.
- [17] R.B. Saffarini, E.K. Summers, H.A. Arafat, and J.H. Lienhard V, Technical evaluation of stand-alone solar powered membrane distillation systems, *Desalination* 286 (2012) 332-341.
- [18] J. Minier-Matar, A. Hussain, A. Janson, F. Benyahia, and S. Adham, Field evaluation of membrane distillation technologies for desalination of highly saline brines, *Desalination* 351 (2014) 101-108.
- [19] H.C. Duong, P. Cooper, B. Nelemans, T.Y. Cath, and L.D. Nghiem, Evaluating energy consumption of membrane distillation for seawater desalination using a pilot air gap system, *Sep. Purif. Technol.* 166 (2016) 55-62.
- [20] D. Winter, Comparative analyses of membrane distillation configurations, PhD Thesis, 2014, pp. 16-17.
- [21] H.C. Duong, A.R. Chivas, B. Nelemans, M. Duke, S. Gray, T.Y. Cath, and L.D. Nghiem, Treatment of RO brine from CSG produced water by spiral-wound air gap membrane distillation - A pilot study, *Desalination* 366 (2015) 121-129.
- [22] R. Schwantes, A. Cipollina, F. Gross, J. Koschikowski, D. Pfeifle, M. Rolletschek, and V. Subiela, Membrane distillation: Solar and waste heat driven demonstration plants for desalination, *Desalination* 323 (2013) 93-106.
- [23] R.G. Raluy, R. Schwantes, V.J. Subiela, B. Peñate, G. Melián, and J.R. Betancort, Operational experience of a solar membrane distillation demonstration plant in Pozo Izquierdo-Gran Canaria Island (Spain), *Desalination* 290 (2012) 1-13.

- [24] H.C. Duong, P. Cooper, B. Nelemans, and L.D. Nghiem, Optimising thermal efficiency of direct contact membrane distillation via brine recycling for small-scale seawater desalination, *Desalination* 374 (2015) 1-9.
- [25] L.D. Nghiem and T. Cath, A scaling mitigation approach during direct contact membrane distillation, *Sep. Purif. Technol.* 80 (2011) 315-322.
- [26] L. Wang, B. Li, X. Gao, Q. Wang, J. Lu, Y. Wang, and S. Wang, Study of membrane fouling in cross-flow vacuum membrane distillation, *Sep. Purif. Technol.* 122 (2014) 133-143.
- [27] J. Gilron, Y. Ladizansky, and E. Korin, Silica fouling in direct contact membrane distillation, *Ind. Eng. Chem. Res.* 52 (2013) 10521-10529.
- [28] E. Curcio, X. Ji, G. Di Profio, A.O. Sulaiman, E. Fontananova, and E. Drioli, Membrane distillation operated at high seawater concentration factors: Role of the membrane on CaCO₃ scaling in presence of humic acid, *J. Membr. Sci.* 346 (2010) 263-269.
- [29] K.L. Hickenbottom and T.Y. Cath, Sustainable operation of membrane distillation for enhancement of mineral recovery from hypersaline solutions, *J. Membr. Sci.* 454 (2014) 426-435.
- [30] M. Gryta, Long-term performance of membrane distillation process, *J. Membr. Sci.* 265 (2005) 153-159.
- [31] P. Zhang, P. Knötig, S. Gray, and M. Duke, Scale reduction and cleaning techniques during direct contact membrane distillation of seawater reverse osmosis brine, *Desalination* 374 (2015) 20-30.
- [32] E. Guillén-Burrieza, J. Blanco, G. Zaragoza, D.-C. Alarcón, P. Palenzuela, M. Ibarra, and W. Gernjak, Experimental analysis of an air gap membrane distillation solar desalination pilot system, *J. Membr. Sci.* 379 (2011) 386-396.
- [33] E. Guillen-Burrieza, A. Ruiz-Aguirre, G. Zaragoza, and H.A. Arafat, Membrane fouling and cleaning in long term plant-scale membrane distillation operations, *J. Membr. Sci.* 468 (2014) 360-372.
- [34] J. Swaminathan, H.W. Chung, D.M. Warsinger, F.A. AlMarzooqi, H.A. Arafat, and J.H. Lienhard V, Energy efficiency of permeate gap and novel conductive gap membrane distillation, *J. Membr. Sci.* 502 (2016) 171-178.
- [35] A.S. Alsaadi, L. Francis, H. Maab, G.L. Amy, and N. Ghaffour, Evaluation of air gap membrane distillation process running under sub-atmospheric conditions: Experimental and simulation studies, *J. Membr. Sci.* 489 (2015) 73-80.
- [36] A. Khalifa, D. Lawal, M. Antar, and M. Khayet, Experimental and theoretical investigation on water desalination using air gap membrane distillation, *Desalination* 376 (2015) 94-108.

- [37] A.S. Alsaadi, N. Ghaffour, J.D. Li, S. Gray, L. Francis, H. Maab, and G.L. Amy, Modeling of air-gap membrane distillation process: A theoretical and experimental study, *J. Membr. Sci.* 445 (2013) 53-65.
- [38] K.W. Lawson and D.R. Lloyd, Membrane distillation, *J. Membr. Sci.* 124 (1997) 1-25.
- [39] R.C. Reid, J.M. Prausnitz, and T.K. Shewood, *The Properties of Gases and Liquids*, McGraw-Hill, New York, 1977.
- [40] M. Wilf and K. Klinko, Optimization of seawater RO systems design, *Desalination* 138 (2001) 299-306.
- [41] A.L. Zydney, Stagnant film model for concentration polarization in membrane systems, *J. Membr. Sci.* 130 (1997) 275-281.
- [42] H. Ozbek, Viscosity of aqueous sodium chloride solutions from 0-150 °C, American Chemical Society 29th Southeast Regional Meeting, Tapa, FL, November 9-11, 1971.
- [43] A. Hausmann, P. Sancio, T. Vasiljevic, U. Kulozik, and M. Duke, Performance assessment of membrane distillation for skim milk and whey processing, *J. Dairy Sci.* 97 (2014) 56-71.
- [44] Y.Z. Tan, J.W. Chew, and W.B. Krantz, Effect of humic-acid fouling on membrane distillation, *J. Membr. Sci.* 504 (2016) 263-273.
- [45] E. Guillen-Burrieza, R. Thomas, B. Mansoor, D. Johnson, N. Hilal, and H. Arafat, Effect of dry-out on the fouling of PVDF and PTFE membranes under conditions simulating intermittent seawater membrane distillation (SWMD), *J. Membr. Sci.* 438 (2013) 126-139.
- [46] F. He, K.K. Sirkar, and J. Gilron, Effects of antiscalants to mitigate membrane scaling by direct contact membrane distillation, *J. Membr. Sci.* 345 (2009) 53-58.
- [47] M. Gryta, Polyphosphates used for membrane scaling inhibition during water desalination by membrane distillation, *Desalination* 285 (2012) 170-176.
- [48] Y. Peng, J. Ge, Z. Li, and S. Wang, Effects of anti-scaling and cleaning chemicals on membrane scale in direct contact membrane distillation process for RO brine concentrate, *Sep. Purif. Technol.* 154 (2015) 22-26.
- [49] J. Ge, Y. Peng, Z. Li, P. Chen, and S. Wang, Membrane fouling and wetting in a DCMD process for RO brine concentration, *Desalination* 344 (2014) 97-107.
- [50] F. He, K.K. Sirkar, and J. Gilron, Studies on scaling of membranes in desalination by direct contact membrane distillation: CaCO₃ and mixed CaCO₃/CaSO₄ systems, *Chem. Eng. Sci.* 64 (2009) 1844-1859.
- [51] M. Gryta, Alkaline scaling in the membrane distillation process, *Desalination* 228 (2008) 128-134.